Cell-Type Variation in Stress Responses as a Consequence of Manipulating GRP78 Expression in Neuroectodermal Cells

Shaun Martin[1], Penny E. Lovat[2], Chris P. F. Redfern[1,*].

[1]*Northern Institute for Cancer Research, Medical School, Newcastle University, NE2 4HH, UK*

[2]*Institute of Cellular Medicine, Medical School, Newcastle University, NE2 4HH, UK*

* To whom correspondence should be addressed:

Dr Chris Redfern

Northern Institute for Cancer Research, Newcastle University

Newcastle upon Tyne

NE2 4HH

United Kingdom.

Telephone: +44 (0) 191 246 4416

Fax: +44 (0) 191 246 4301

E-mail: **chris.redfern@ncl.ac.uk**

Running Title: GRP78 and stress response in neuroectodermal cancer cells

KEYWORDS: GRP78; STRESS; ENDOPLASMIC RETICULUM STRESS;

NEUROBLASTOMA; MELANOMA

Total number of text figures: 8; no tables.

Grant sponsor: Cancer Research UK, grant number C1376/A9254.

ABSTRACT

Glucose-regulated protein 78 (GRP78) is a stress sensor which interacts with unfolded protein response (UPR) activators in the endoplasmic reticulum (ER). The aim of this study was to test the hypothesis that GRP78 has distinct functional roles in mediating the effects of ER stress in neuroblastoma compared to other neuroectodermal cancer types. GRP78 was knocked down or overexpressed in neuroectodermal tumour cell lines. Protein and transcript expression were measured using Western blotting, confocal microscopy and real-time polymerase chain reaction; cell stress was assessed by measurement of oxidative stress and accumulation of ubiquitinated proteins and cell response by measurement of apoptosis and cell viability. Neuroblastoma cells were more sensitive to ER stress than melanoma and glioblastoma cells. GRP78 knockdown increased stress sensitivity of melanoma and glioblastoma cells, but not neuroblastoma cells. Over-expression of GRP78 decreased the stress sensitivity of melanoma and glioblastoma cells but, in contrast, increased the stress sensitivity of neuroblastoma cells by activation of caspase-3-independent cell death and substantially increased the expression of UPR activators, particularly inositol-requiring element 1 (IRE1). The results from this study suggest that cell-type specific differences in the relationships between GRP78 and the UPR activators, particularly IRE1, may determine differential sensitivity to ER stress.

Survival in heterogeneous microenvironments is a defining characteristic of metastatic tumour cells, and relies on an ability to adapt to varying degrees and types of stress [Kenific et al., 2010]. Understanding how to abrogate selectively the homeostatic mechanisms allowing cancer cells to survive outside their normal tissue environment is important for developing strategies to limit metastasis. The endoplasmic reticulum (ER) has a key role in sensing stress and in providing the scaffold, quality control and redox environment for correctly assembling newly-synthesised proteins. Disrupting ER function leads to the accumulation of unfolded or mis-folded proteins and activation of the Unfolded Protein Response (UPR), a homeostatic mechanism which may represent a target for controlling tumour metastasis. In this context, the protein-folding chaperone glucose-regulated protein 78 (GRP78) has a key role in sensing ER stress and facilitating adaptive responses.

GRP78 has high affinity for unfolded or mis-folded proteins and interactions with such substrates result in its dissociation from the UPR activators Protein kinase-like ER kinase (PERK), Inositol-Requiring Element 1 (IRE1) and Activating Transcription Factor 6 (ATF6) [Schroder, 2006]. PERK release facilitates kinase activation by autophosphorylation-induced homodimerisation, leading to attenuation of general protein synthesis [Bertolotti et al., 2000; Harding et al., 1999], while allowing translation of mRNA for pro-survival and pro-death stress-response proteins [Harding et al., 2000]; these proteins include Activating Transcription Factor 4 (ATF4), which in turn stimulates synthesis of chaperones, including GRP78, other proteins involved in homeostasis [Fels, 2006] and, under prolonged or severe stress, the pro-apoptotic transcription factor growth arrest and DNA damage induced gene 153 (GADD153) [Wing et al., 1996]. Negative feedback inhibition of PERK, and eIF2α de-phosphorylation [Kebache et al., 2004; Van Huizen et al., 2003] as stress is resolved, restores normal translation capacity.

Once released from GRP78, oligomerization and autophosphorylation of IRE1, a trans-membrane protein kinase endoribonuclease, results in RNase-domain activation and splicing of mRNA for X-box binding protein 1 (XBP-1). Downstream events of IRE1 activation include regulation of ER-resident chaperones and promotion of death via activation of GADD153and c-Jun N-terminal kinase (JNK) [Urano et al., 2000]. IRE1 also phosphorylates tumour necrosis factor receptor 2 (TRAF2) leading to activation of JNK and caspase-independent apoptosis via Bax and pro-apoptotic factors [Kroemer et al., 2007]. ATF6 released from GRP78 is cleaved in the Golgi to an active transcription factor which binds to promoters containing ER-stress response elements and regulates expression of ER-stress-related proteins such as GRP78, XBP-1 and GADD153 [Yoshida et al., 2000]. Although PERK, IRE1 and ATF6 appear to have separate roles in stress signalling, ATF6 has functional overlap with PERK and IRE1 signalling pathways.

Recent studies to understand the cellular role of GRP78 in tumour cells have suggested that increased GRP78 expression in melanoma and glioblastoma promotes cell survival and correlates with poor prognosis [Hersey and Zhang, 2008; Lee et al., 2008; Liquing et al., 2009]; conversely, increased GRP78 expression in neuroblastoma may correlate with greater stress sensitivity and better prognosis [Hsu et al., 2005]. These conflicting reports imply that GRP78 has different roles as a sensor of ER stress in different types of neuroectodermal tumours. The aim of this study was to test the hypothesis that GRP78 has functionally- or mechanistically-distinct roles in mediating the effects of ER stress in neuroblastoma compared to other neuroectodermal cell types.

MATERIALS AND METHODS

GROWTH AND MAINTENANCE OF CELL LINES

SH-SY5Y and NGP human neuroblastoma cells were cultured in RPMI 1640, 10% foetal bovine serum (FBS). U251 and MO59J human glioblastoma and CHL-1 and WM266-4 (ATCC #; CRL-9446, CRL-1676) human melanoma cells were cultured in high glucose (4.5 g/L) DMEM, 10% FBS. All media were from Sigma-Aldrich (Poole, UK). Cells were regularly tested for mycoplasma and maintained at 37 °C, 5% CO_2 in air (humidified), for up to 50 passages. Bortezomib (Janssen Cilag Ltd, High Wycombe, UK) was added to cultures in DMSO, and fenretinide (Janssen-Cilag, Switzerland) in ethanol.

CELL DEATH

Seeding densities (cells per well) for overnight attachment in flat-bottomed 6-well plates were 1.5 x 10^5 for CHL-1, 2.0 x 10^5 for U251, MO59J, SH-SY5Y and NGP, and 2.5 x 10^5 for WM266-4 cells. FACScan or FACScalibur flow cytometers (Becton Dickinson Immunocytometry systems, Oxford, UK) were used to record the percentage of propidium iodide-stained cells with hypodiploid DNA (subG1 peak) as a measure of cell death as described previously [Lovat et al., 2008; Lovat et al., 2004].

ANALYSIS OF CELLULAR PROTEINS

Proteins were analysed by gel electrophoresis and Western blotting, using β-actin as a reference after loading in each gel lane equivalent amounts of protein or protein from the same number of cells. Protein was measured with a Bradford assay (Pierce Biotech., Rockford, IL) using a bovine serum albumin (BSA) standard; cells were counted using a Vi-Cell counter (Beckman Coulter, Dunstable, UK). Cell lysates were prepared and analysed by Western blotting using 4-20% Tris-glycine polyacrylamide gels (Bio-Rad laboratories, Hemel Hempstead, UK) as described previously [Armstrong et al., 2007]. Antibodies and dilutions used to probe blots were for the GRP78 C-Terminus (Santa Cruz, sc1051; 1:1000 dilution), Cleaved Caspase 3 (Cell Signalling, 9661L; 1:500), PERK (Santa Cruz, sc9481; 1:2000), IRE1 α (Santa Cruz, sc20790; 1:2000), ATF6 α (Santa Cruz, sc-14253; 1:500), ATF4 (Calbiochem, PC715; 1:500), , , Ubiquitin (Cell Signalling [P4D1], #3936; 1:1000) and β-actin (Sigma-Aldrich, A2228; 1:5000). Horseradish peroxidase-conjugated secondary antibodies (Upstate Biotechnology, Boston, USA; diluted 1:2000) were used for detection with the ECL-plus system (Amersham Biosciences, Little Chalfont, UK) with imaging on a Fujifilm FLA-3000 fluorescence imager (Raytek Scientific Ltd, Sheffield, UK). Aida Image Analyser version 3.28 was used for densitometric quantification relative to control treatments. For ATF4, data were expressed as 'attomoles/cell' (amoles/cell) by reference to a standard consisting of a 26 kDa His-tagged ATF4 fragment consisting of amino acids 123-351from Abcam (Cambridge, UK). Estimates of cell and nuclear diameters were obtained from phase contrast images and 4',6-diamidino-2-phenylindole (DAPI) -stained confocal microscopy images of detached spherical cells. Cytosolic concentrations of ATF4 were then estimated using the mean cytosolic volumes calculated from mean cell and nuclear diameters of detached cells.

FLOW CYTOMETRY FOR THE INDUCTION OF REACTIVE OXYGEN SPECIES (ROS)

Cells were seeded into 6-well plates (as above) before treatment with ER stress-inducing agents over a 6 h time course. After treatment, culture medium was removed and cells washed twice in PBS before harvesting by trypsinisation, pelleted by centrifugation at 330 *g* for 5 min and resuspended in 500 µl of 5 µM 5-(and-6)-Carboxy-2',7'-Dichlorofluorescein Diacetate (DCFDA, Sigma-Aldrich). Samples were then incubated at 37 °C for 15 min, washed twice in ice-cold PBS by centrifugation and stored on ice for analysis by flow cytometry. Negative controls were unstained cells and working dye solution alone, and

positive controls were cells treated with 25 µM and 50 µM hydrogen peroxide for 6 h (Sigma-Aldrich). Flow cytometry data were collected using CellQuest v. 3.3 software using a gated amplifier for FL1 (λ 530/30 nm; fluorescein) and a signal threshold for forward and side scatter to exclude debris.

SMALL INTERFERING RNA (SIRNA)-MEDIATED KNOCKDOWN OF GRP78

Knockdown of GRP78 was performed using a double-transfection procedure as described by Martin et al (2010) [Martin et al., 2010] using GRP78 siRNA (Hs_HSPA5_6_HP validated siRNA; Qiagen, Crawley, UK) or control scrambled siRNA (Qiagen). Knockdown was verified by Western blot 24 h after the second transfection or when subsequent cell viability and death assays were performed.

REVERSE TRANSCRIPTASE QUANTITATIVE POLYMERASE CHAIN REACTION (RT-QPCR)

Cells were washed (PBS), detached and pelleted by centrifugation, washed once with PBS and total RNA extracted using the RNeasy Kit (Qiagen). To prepare cDNA, 0.5 µg RNA was combined with 0.5 µg random oligo dT primers, 0.5 mM deoxynucleotide triphosphates (dNTPs), and RNase-free water (final volume 20 µl), and incubated at 65 °C for 5 min followed by 1 min on ice; 4 µl of first-strand buffer, 1 µl of 0.1 M DTT, 1 µl of RNase Inhibitor and 1 µl of Superscript Reverse Transcriptase were added and incubated at 55 °C for 60 min before terminating the reaction at 70 °C for 15 min. RNase H (0.5 µl of 5U/µl stock) was added, incubated for 20 min at 37 °C and inactivated at 65 °C for 10 min. All reagents were from Fermentas (St. Leon-Rot, Germany). Real-time PCR reactions (20 µl volume) were carried out in triplicate reactions with PCR primers for GRP78 (GTT CTT GCC GTT CAA GGT GG and TGG TAC AGT AAC AAC TGC ATG) and or β-Actin control (AAT CTG GCA CCA CAC CTT CTA CA and CGA CGT AGC ACA GCT TCT CCT TA) and a 2 x concentration of fast SYBR green master mix containing AmpliTaq fast DNA polymerase, SYBR Green-1 dye and dNTPs with an Applied Biosystems 7500 fast real-time PCR machine with SDS software (Applied Biosystems, Carlsbad, California, USA). PCR conditions were an initial denaturation at 95 °C (10 min), 50 cycles of 15 s at 95 °C and 60 s at 60 °C for GRP78 or 15 s at 95 °C, 45 s at 60 °C and 30 s at 72 °C for β-actin followed by a final cycle of 30 s at 95 °C and 60 s at 60 °C.

STABLE OVER-EXPRESSION OF GRP78

Plasmid DNA pcDNA3.0 or pcDNA3.1 (+) containing full-length GRP78 cDNA (a gift from Randal Kaufman) were transfected into WM266-4, MO59J and NGP cells in 6-well plates at 3.0×10^5 cells per well. Plasmid DNA (4 µg in 8 µl) and 12 µl of Lipofectamine 2000 transfection reagent (Invitrogen, Paisley, UK) were mixed separately with 500 µl OptiMEM medium (Invitrogen), combined together at room temperature for 15 min and then diluted with 1.5 ml OptiMEM. Culture medium was removed from the cells, the cells washed with OptiMEM and then incubated with the transfection mixture for 24 h at 37 °C. Medium was then replaced with 3 ml of culture medium containing 10% FBS and 2 mM L-glutamine, and incubated for 48 h at 37 °C before selection with geneticin (G418; Invitrogen) at 1500 µg/ml for neuroblastoma cells and 2000 µg/ml for melanoma and glioblastoma cells. Transfected cells were maintained under G418 selection over 10 passages as a mixed population without clonal selection. For experiments, cells were placed in normal culture media for a minimum of 3 days prior to the start of each experiment.

CONFOCAL MICROSCOPY

Cells were fixed in 100% ice-cold methanol (Fisher; 30 min), washed in PBS containing 0.05% Tween 20 (PBS/T; Sigma-Aldrich) and permeabilised in 0.2% Triton X100 (Sigma-Aldrich, diluted in PBS/T) for 30 min. After blocking with 2% BSA in PBS/T for 1 h, samples were washed thrice in PBS/T and incubated with GRP78 primary antibody (Santa Cruz; 1:500), in 0.2% BSA-PBS/T for 1 h at room temperature. After washing 3 times in PBS/T, blocking in 10% secondary host-antibody-specific serum in PBS/T for 30 min, samples were incubated with fluorescently-labelled secondary antibodies diluted in 1% host-specific serum for 1 h. Cell nuclei were stained with 4',6-diamidino-2-phenylindole (DAPI; Sigma-Aldrich) diluted in PBS/T for 25 min. Stained cells were mounted in Vector Shield mounting medium (Vector Laboratories LTD, Peterborough, UK) and imaged within 24 h using a x48 objective on a Zeiss LSM 700 inverted confocal scanning microscope (Zeiss, Hertfordshire, UK) with averaging of 4 and a frame size of 1024 x 1024 pixels. Each experiment included a negative control of unstained cells, as well as secondary antibody only to control for non-specific binding. Laser power, optimised on control- stained cells, remained the same throughout each experiment.

DATA ANALYSES

Flow cytometry data were analysed using either WinMDI 2.8 for flow cytometry (Bio-soft.net) or Cyflogic 1.2.1 (Cyflogic, Turku, Finland). Real time PCR data were analysed using SDS2.2 software (Applied Biosystems). The threshold level of expression was set to a value on the exponential phase of amplification plots and kept the same for all related primer-probe experiments. The PCR cycles taken to reach the threshold (Ct) for each sample was generated as mean ± 95% confidence intervals (CI) normalised to the β-Actin control data and then to the vehicle-treated control samples. Experimental data were expressed as the mean of individual experiments ± 95% confidence intervals (95% CI) using Prism 5 (GraphPad Software Inc; La Jolla, CA, USA) or Sigma Plot 11 (Systat Software Inc; San Jose, CA, USA) software. Responses were compared by one- or two-way ANOVA with either Dunnett's or the more-conservative Bonferroni's post-hoc tests using Prism 5, SPSS release 17.0 (IBM; Chicago, IL, USA) or R software. Error bars on all graphs are 95% confidence intervals. Dose response parameters were fitted using R and the package drc [Ritz and Streibig, 2005].

RESULTS

RESPONSES TO STRESS-INDUCING AGENTS IN NEUROECTODERMAL CELL LINES

For this work, we studied six cell lines in parallel: two melanoma (CHL1, WM266-4), two glioblastoma (U251, MO59J) and two neuroblastoma (SH-SY5Y, NGP) cell lines. Fenretinide and bortezomib induce ER stress in melanoma and neuroblastoma cells [Hill et al., 2009; Pagnan et al., 2009] by oxidative stress [Lovat et al., 2000] and 26S proteasome inhibition, respectively. For the six cell lines, sensitivity and responses to fenretinide and bortezomib were characterised in terms of cell death at 24 h and the induction of the stress marker ATF4 after 4 h of treatment. For neuroblastoma and melanoma cells, dose-response data indicated maximum cell death of 30-50% but differing sensitivities between cell types with 10-fold lower concentrations of bortezomib and 2-fold lower concentrations of fenretinide required for neuroblastoma cells (Figure 1A). Conversely, glioblastoma cells had higher levels of death (up to 80%; Figure 1A) but within a similar sensitivity range to melanoma cells. ATF4 induction was evident in all cell lines but to differing levels and was induced to 3- to 10-fold higher levels in melanoma cells compared to neuroblastoma cells with intermediate levels of induction observed for glioblastoma cells (Figure 1B).

With doses in the mid-range of response, fenretinide rapidly induced reactive oxygen species (ROS) in all six cell lines, reaching a plateau after 2-4 h but at higher steady-state levels in melanoma than neuroblastoma cells and, again, intermediate values in glioblastoma cells (Figure 2A). ATF4 was induced by fenretinide over a similar time course, rather more transiently in melanoma cells but remaining elevated in glioblastoma cells (Figure 2B), and to lower levels in neuroblastoma cells. In response to bortezomib, ubiquitin decreased and ubiquitinated proteins increased steeply during the first 8 h (Figure 2C, E). Greatest increases in ubiquitinated proteins, relative to the zero h controls, were produced in glioblastoma cells, reaching 20-fold by 24 h, with lower levels in melanoma cells (8- to 10-fold increase by 24 h) and very small increases in neuroblastoma cells (1.5-fold increase by 8-24 h; Figure 2C,E). ATF4 increased over a similar time scale, reaching a peak by 4-8 h and remaining substantially elevated until at least 24 h (Figure 2D).

CELL DEATH AFTER GRP78 KNOCKDOWN

To test the role of GRP78 in drug and stress sensitivity, GRP78 expression was reduced by RNA interference. We have previously reported the siRNA-mediated knockdown of GRP78 in CHL-1 and WM266-4 cells [Martin et al., 2010] and used the same technique to achieve a modest reduction in GRP78 expression of > 50% in all cell lines, ranging from 56.3% in CHL-1 cells [Martin et al., 2010] to 82.3% in U251 glioblastoma cells. Treatment with fenretinide or bortezomib resulted in the induction of GRP78 as part of the stress response, and this was abrogated after knockdown of GRP78 (Figure 3 and [Martin et al., 2010]).

Knockdown of GRP78 increases cell death of melanoma cells in response to fenretinide or bortezomib [Martin et al., 2010]. For glioblastoma cells, GRP78 knockdown also resulted in statistically-significant increases in death in response to fenretinide or bortezomib (Figure 3A, B), similar to melanoma cells. Conversely, death was not significantly increased in either of the neuroblastoma cell lines (Figure 3C, D) and there was a small but statistically-significant decrease in death of fenretinide-treated SH-SY5Y cells (Figure 3D). These results were confirmed in experiments to measure the effect of GRP78 knock-down on stress-induced inhibition of cell viability (Figure S1).

Increased sensitivity to stress would be predicted from GRP78 knockdown, but in view of the fact that GRP78 interacts directly with the stress sensors, it is important to ask if there are correlated or compensatory alterations in expression of PERK, IRE1 and ATF6 as a result of GRP78 knockdown. For melanoma cells, there was no apparent effect on GRP78 knockdown on ATF6 or PERK expression but a 1.3-fold increase in IRE1 expression (Figure 4A). UPR activator expression overall was reduced slightly (by up to 0.9-fold) in glioblastoma cells (Figure 4B). Conversely, there were no significant changes in UPR activator levels in the neuroblastoma cells in response to GRP78 knockdown (Figure 4C). Overall, the magnitudes of changes in UPR activator levels were small in comparison to the > 50% knockdown of GRP78.

RESISTANCE AND SENSITIVITY TO STRESS AFTER OVER-EXPRESSION OF GRP78

To test the prediction that increasing GRP78 expression would increase resistance to stress, GRP78 was stably over-expressed in one cell line of each type: WM266-4 melanoma, MO59J glioblastoma and NGP neuroblastoma cells. Compared to cells stably transfected with empty vector, in GRP78-transfected cells, GRP78 mRNA was increased 1.5- to 2-fold. Similarly, GRP78 protein increased by 1.7-fold in melanoma, 1.96-fold in glioblastoma and 1.5-fold in the neuroblastoma cells (Figure 5A, B) and this was confirmed by confocal microscopy which also showed increased GRP78 staining with similar intracellular distributions to control cells (Figure 5C, D).

Unlike WM266-4 and MO59J cells, over-expression of GRP78 in NGP neuroblastoma cells resulted in morphological changes: cells increased in size with a decrease in dendrites and an increase in detachment (Figure 6A, B). Over-expression of GRP78 in all three cell lines affected sensitivity to fenretinide or bortezomib with reduced death in WM266-4 and MO59J cells (Figure 6C, D). However, NGP neuroblastoma cells showed increased sensitivity to stress and the death of the vehicle-treated control cells was increased compared to vector-transfected or wild-type cells (Figure 6E). These effects, although relatively small, were mirrored by increased viability of WM266-4 and MO59J cells over-expressing GRP78 and treated with fenretinide or bortezomib, but decreased viability of NGP cells under the same conditions (Figure S2). For confirmation of effects on neuroblastoma cells, we transiently over-expressed GRP78 in NGP cells in the absence of ER stress. Death of these cells was increased in a GRP78-dose-dependent manner 24 h after transfection (Figure 6F) and confirmed the results from stable over-expression experiments that, contrary to prediction, higher levels of GRP78 expression increased neuroblastoma cell death and reduced survival.

With respect to biochemical markers of cell stress and death, the induction of ATF4 and cleavage of caspase-3 in response to fenretinide or bortezomib were measured (Figure 7A-C). In stressed WM266-4 and MO59J cells overexpressing GRP78, ATF4 induction and caspase-3 cleavage were significantly reduced. Conversely, the over-expression of GRP78 increased ATF4 induction in NGP neuroblastoma cells treated with bortezomib but decreased ATF4 induction in response to fentretinide compared to control vector-transfected cells; unexpectedly, however, caspase-3 cleavage in these NGP cells was also reduced in response to both drugs, despite the increased levels of cell death (Figure 6) produced under these conditions.

For all three cell types there were no significant differences in UPR activator expression between wild-type cells and those stably transfected with empty vector; in contrast, IRE1 expression was increased 2-fold in WM266-4 cells over-expressing GRP78 and accompanied by a small decrease in ATF6 expression (Figure 7D,E). In MO59J cells over-expressing GRP78, PERK expression was reduced by 50% whereas for NGP cells, GRP78 over-expression resulted in increased levels of all three UPR activators, with marked ≈3-fold increases in IRE1 and ATF6, as well as a small increase in PERK.

STRESS AFTER GRP78 OVER-EXPRESSION

These results provide evidence that neural-crest-derived tumour cell types differ in how stress-sensor functions of GRP78 are modulated to determine the outcome of stress. Given the dynamic nature of cellular homeostatic control, it is important to ask if stress apparently experienced by cells is altered by GRP78 over-expression. In WM266-4 and MO59J cells stably over-expressing GRP78, fenretinide-induced ROS was inhibited; however, this was not the case when GRP78 was over-expressed in NGP neuroblastoma cells (Figure 8A). With respect to cells treated with bortezomib, the accumulation of ubiquitin-tagged proteins was reduced by GRP78 over-expression in WM266-4 and MO59J cells (Figure 8B) but increased in NGP cells. Thus, reduced death in response to bortezomib in cells over-expressing GRP78 was associated with a reduced ability of bortezomib to inhibit 26S proteasome activity. Conversely, although fenretinide-induced ROS and death were reduced in melanoma and glioblastoma cells by over-expressing GRP78, in neuroblastoma cells the higher levels of fenretinide-induced death with GRP78 over-expression were not accompanied by increased ROS (Figure 8A).

DISCUSSION

Fenretinide and bortezomib both activate the PERK/ATF4 arm of the UPR [Lai and Wong, 2008; Obeng et al., 2006] but do so to differing extents. The steady accumulation of ubiquinated proteins induced with bortezomib implies a sustained effect with stress increasing over time, reflected by the high and continued expression of the ER stress-inducible marker ATF4. In contrast, ROS induced by fenretinide reached a maximum after only a few hours and induced a transient ATF4 expression, implying adaptation to higher ROS levels. Despite apparent differences in mechanisms, levels of death induced by each agent were apparently cell-type specific. Although we discuss our data in the context of intracellular GRP78, some studies have suggested that using antibodies to modulate activity of cell-surface GRP78 may affect stress sensitivity [Liu et al., 2013; Misra et al., 2009]. However, we have been unable to demonstrate (Martin, Lovat, Redfern unpublished data) a convincing effect of an anti-GRP78 antibody on increasing the sensitivity of melanoma, glioblastoma or neuroblastoma cells to stress-inducing drugs. Therefore, it is likely that the role of GRP78 in the context of our studies is mediated by intracellular signalling pathways.

Reducing GRP78 expression may increase stress sensitivity, perhaps by reduced chaperone capacity or by priming the UPR as a consequence of excess unbound UPR activators. As with the melanoma and glioblastoma cell lines used for this study, increased stress sensitivity resulting from reductions in GRP78 expression has also been reported for breast cancer and HeLa cells [Cook et al., 2012; Suzuki et al., 2007]. The consequence of GRP78 knockdown is likely, on the basis of simple mass-action models of the association and dissociation kinetics of GRP78 with each of the UPR activators, to lead to increases in levels of free IRE1, PERK and ATF6. Although IRE1 can have pro-survival and pro-apoptotic functions, such potential changes in UPR activators could drive increased sensitivity of cells to stress. However, neuroblastoma cells did not show increased sensitivity to stress after GRP78 knockdown, implying a contextual relationship between GRP78, UPR activators and stress sensitivity.

The converse experiment, increasing GRP78 levels by stable over-expression, produced the predicted result in WM266-4 melanoma and MO59J glioblastoma cells, reducing death in response to stress. In contrast to transient knockdown experiments, stable over-expression of GRP78 was accompanied by variable but relatively large changes in UPR activator expression, with reductions in PERK in the glioblastoma cells and increased IRE1 but decreased ATF6 in melanoma cells. The contribution of these changes in UPR activator expression to decreased stress sensitivity is uncertain because GRP78 over-expression in these cells was also accompanied by reduced stress in response to fenretinide or bortezomib. In marked contrast, GRP78 over-expression in the NGP neuroblastoma cells increased stress-induced death, possibly as a result of the large and unexpected increases in expression of all three UPR activators. There was also a marked phenotypic change in these cells which may indicate a functional role for GRP78 in morphogenesis and differentiation, either directly [Barnes and Smoak, 2000] or as a result of changes in expression of UPR activators, particularly IRE1 or downstream transcription factors such as XBP1 [Cho et al., 2013], or interaction with other chaperones [Gunter and Degnan, 2007].

GRP78 is involved in the regulation of redox levels as a stress response via the PERK-dependent activation of Nrf2 and up-regulation of redox-defensive genes [Cullinan et al., 2003; Niture et al., 2010]. Others have shown that GRP78 knockdown can increase endogenous ROS levels, but subsequent effects of stress-inducing agents are unpredictable [Chang et al., 2012]. Therefore, reduction in ROS in melanoma and glioblastoma cells over-expressing GRP78 and treated with fenretinide is consistent with a role of GRP78 in redox regulation, although whether mediated directly by GRP78 or indirectly via PERK is unknown. Reductions in bortezomib-induced accumulation of ubiquitinated proteins in melanoma and glioblastoma cells over-expressing GRP78 may result from an increase in

chaperone capacity. GRP78 may have a role in ERAD by interacting with the E3 Ubiquitin ligase HRD-1 [Sasagawa et al., 2007] and a ubiquitin hydrolase [Fang et al., 2012]; such interactions in cells over-expressing GRP78 could decrease the accumulation of ubiquitinated proteins in response to bortezomib. GRP78 can also inhibit caspases mediating ER-stress-induced apoptosis [Reddy et al., 2003], an additional mechanism that could lead to decreased stress sensitivity of WM266-4 and MO59J cells over-expressing GRP78, and to increased sensitivity under knockdown conditions. Thus, in melanoma and glioblastoma cells under conditions of high GRP78 expression, reduced stress sensitivity may result from reductions in free UPR activators (predicted by considering mass-action relationships), caspase inhibition and reduced levels of stress (greater first-line stress defences); conversely, after GRP78 knockdown, higher levels of free UPR activators and low caspase inhibition, potentially coupled with reduced stress defences, would increase stress sensitivity.

GRP78 seems to act as a buffer for regulating IRE1 activity [Pincus et al., 2010] and for neuroblastoma cells it is possible that the effect of manipulating GRP78 levels may be driven by IRE1 and interactions coupling IRE1 to death pathways other than the PERK/ATF4 axis. Levels of ubiquitinated-protein accumulation in these cells were, compared to melanoma and glioblastoma cells, high under basal conditions and changed little in response to bortezomib. As well as binding to GRP78, IRE1 interacts with HRD-1 [Gao et al., 2008], presenilin-1 [Niwa et al., 1999], TRAF2 [Urano et al., 2000], TAO kinase 3 [Yoneda et al., 2001] and MAP3K5 (ASK1) [Nishitoh et al., 2002]. TRAF2, TAO Kinase 3 and ASK1 are components of the ASK1-JNK pathway leading to apoptosis by both caspase-dependent and -independent mechanisms; in neuronal cells, caspase-independent apoptosis via a kinase-independent ASK1/Daxx interaction [Charette et al., 2001] and JNK-dependent pathways [Kamalden et al., 2012] have been described. As caspase-3 cleavage was not a feature of increased stress-induced cell death in NGP cells over-expressing GRP78, apoptosis under these conditions may be driven by caspase-3-independent processes resulting from increased IRE1 levels. IRE1 is also a component of the ERAD/ubiquitination system via its interaction with HRD-1 [Gao et al., 2008] and in the transcriptional regulation of ERAD components [Lee et al., 2003]; therefore, increased accumulation of ubiquitinated proteins in bortezomib-treated cells may also result from higher IRE1 levels.

It is clear from this and other studies that GRP78 has complex roles in cell signalling, stemming from its interactions from the three stress sensors as well as with other proteins. In breast cancer cells, apoptosis may be regulated by interactions between GRP78 and the pro-apoptotic BH3-domain protein Bik [Zhou et al., 2011]; thus, changes in the availability of free Bik as a result of GRP78 over-expression or knockdown could be a contributory factor to the increased resistance or sensitivity, respectively, seen in melanoma and glioblastoma cells. Nevertheless, the results from this study suggest that cell-type specific differences in the relationships between GRP78 and the UPR activators, particularly IRE1, may determine differential sensitivity to ER stress. For IRE1 there are likely to be complex relationships between monomer (kinase inactive) IRE1, active IRE1 oligomers, GRP78 and IRE1-interacting proteins such as TRAF2, HRD-1, ASK1 and TAO Kinase 3 and interpreting the outcome of changes in expression of one or more of these components will require computational approaches to couple signalling fluxes to cellular outcome in terms of adaptation (homeostasis/repair) or cell death, coupled with experimental measurements of stoichiometric relationships between GRP78 and UPR activators in relation to stress sensitivity.

Supporting information

Figure S1

Figure S2

ACKNOWLEDGEMENTS

We thank Olaf Heidenreich and Randal Kaufman for their generous gifts of plasmids. This research was funded by a William Ross PhD studentship from Cancer Research UK and we are very grateful for their support.

REFERENCES

Armstrong JL, Veal GJ, Redfern CPF, Lovat PE. 2007. Role of Noxa in p53-independent fenretinide-induced apoptosis of neuroectodermal tumours. Apoptosis 12:613-622.

Barnes JA, Smoak IW. 2000. Glucose-regulated protein 78 (GRP78) is elevated in embryonic mouse heart and induced following hypoglycemic stress. Anat Embryol 202:67-74.

Bertolotti A, Zhang Y, Hendershot LM, Harding HP, Ron D. 2000. Dynamic interaction of BiP and ER stress transducers in the unfolded-protein response. Nat Cell Biol 2:326-32.

Chang YJ, Huang YP, Li ZL, Chen CH. 2012. GRP78 knockdown enhances apoptosis via the down-regulation of oxidative stress and Akt pathway after epirubicin treatment in colon cancer DLD-1 cells. PLoS One 7:e35123.

Charette SJ, Lambert H, Landry J. 2001. A kinase-independent function of Ask1 in caspase-independent cell death. J Biol Chem 276:36071-4.

Cho YM, Kim DH, Kwak SN, Jeong SW, Kwon OJ. 2013. X-box binding protein 1 enhances adipogenic differentiation of 3T3-L1 cells through the downregulation of Wnt10b expression. FEBS Lett 587:1644-9.

Cook KL, Shajahan AN, Warri A, Jin L, Hilakivi-Clarke LA, Clarke R. 2012. Glucose-regulated protein 78 controls cross-talk between apoptosis and autophagy to determine antiestrogen responsiveness. Cancer Res 72:3337-49.

Cullinan SB, Zhang D, Hannink M, Arvisais E, Kaufman RJ, Diehl JA. 2003. Nrf2 is a direct PERK substrate and effector of PERK-dependent cell survival. Mol Cell Biol 23:7198-209.

Fang Y, Mu J, Ma Y, Ma D, Fu D, Shen X. 2012. The interaction between ubiquitin C-terminal hydrolase 37 and glucose-regulated protein 78 in hepatocellular carcinoma. Mol Cell Biochem 359:59-66.

Fels DR. 2006. The PERK/eIF2alpha/ATF4 module of the UPR in hypoxia resistance and tumour growth. Cancer Biol Ther 5:723-8.

Gao B, Lee SM, Chen A, Zhang J, Zhang DD, Kannan K, Ortmann RA, Fang D. 2008. Synoviolin promotes IRE1 ubiquitination and degradation in synovial fibroblasts from mice with collagen-induced arthritis. EMBO Rep 9:480-5.

Gunter HM, Degnan BM. 2007. Developmental expression of Hsp90, Hsp70 and HSF during morphogenesis in the vetigastropod Haliotis asinina. Dev Genes Evol 217:603-12.

Harding HP, Novoa I, Zhang YH, Zeng HQ, Wek R, Schapira M, Ron D. 2000. Regulated translation initiation controls stress-induced gene expression in mammalian cells. Mol Cell 6:1099-1108.

Harding HP, Zhang Y, Ron D. 1999. Protein translation and folding are coupled by an endoplasmic-reticulum-resident kinase. Nature 379:271-4.

Hersey P, Zhang XD. 2008. Adaptation to ER stress as a driver of malignancy and resistance to therapy in human melanoma. Pigment Cell Mel Res 21:358-367.

Hill DS, Martin S, Amnstrong JL, Flockhart R, Tonison JJ, Simpson DG, Birch-Machin MA, Redfern CPF, Lovat PE. 2009. Combining the Endoplasmic Reticulum Stress-Inducing Agents Bortezomib and Fenretinide as a Novel Therapeutic Strategy for Metastatic Melanoma. Clin Cancer Res 15:1192-1198.

Hsu WM, Hsieh FJ, Jeng YM, Kuo ML, Tsao PN, Lee H, Lin MT, Lai HS, Chen CN, Lai DM, Chen WJ. 2005. GRP78 expression correlates with histologic differentiation and favorable prognosis in neuroblastic tumors. Int J Cancer 113:920-7.

Kamalden TA, Ji D, Osborne NN. 2012. Rotenone-induced death of RGC-5 cells is caspase independent, involves the JNK and p38 pathways and is attenuated by specific green tea flavonoids. Neurochem Res 37:1091-101.
Kebache S, Cardin E, Larose L. 2004. Nck-1 antagonizes the endoplasmic reticulum stress induced inhibition of translation. J Biol Chem 279:9662-9671.
Kenific CM, Thorburn A, Debnath J. 2010. Autophagy and metastasis: another double-edged sword. Curr Opin Cell Biol 22:241-5.
Kroemer G, Galluzzi L, Brenner C. 2007. Mitochondrial membrane permeabilization in cell death. Physiol Rev 87:99-163.
Lai WL, Wong NS. 2008. The PERK/eIF2 alpha signaling pathway of Unfolded Protein Response is essential for N-(4-hydroxyphenyl)retinamide (4HPR)-induced cytotoxicity in cancer cells. Exp Cell Res 314:1667-82.
Lee AH, Iwakoshi NN, Glimcher LH. 2003. XBP-1 regulates a subset of endoplasmic reticulum resident chaperone genes in the unfolded protein response. Mol Cell Biol 23:7448-59.
Lee HK, Xiang C, Cazacu S, Finniss S, Kazimirsky G, Lemke N, Lehman NL, Rempel SA, Mikkelsen T, Brodie C. 2008. GRP78 is overexpressed in glioblastomas and regulates glioma cell growth and apoptosis. Neuro-Oncol 10:236-243.
Liquing Z, Richard AS, Lee CS, Stanley WM, Wendy AC, Xu DZ, John FT, Peter H. 2009. Expression of glucose-regulated stress protein GRP78 is related to progression of melanoma. Histopathol 54:462-470.
Liu R, Li X, Gao W, Zhou Y, Wey S, Mitra SK, Krasnoperov V, Dong D, Liu S, Li D, Zhu G, Louie S, Conti PS, Li Z, Lee AS, Gill PS. 2013. Monoclonal antibody against cell surface GRP78 as a novel agent in suppressing PI3K/AKT signaling, tumor growth, and metastasis. Clinical cancer research : an official journal of the American Association for Cancer Research 19:6802-11.
Lovat PE, Corazzari M, Armstrong JL, Martin S, Pagliarini V, Hill D, Brown AM, Piacentini M, Birch-Machin MA, Redfern CPF. 2008. Increasing melanoma cell death using inhibitors of protein disulfide isomerases to abrogate survival responses to endoplasmic reticulum stress. Cancer Res 68:5363-9.
Lovat PE, Corazzari M, Goranov B, Piacentini M, Redfern CPF. 2004. Molecular mechanisms of fenretinide-induced apoptosis of neuroblastoma cells. Ann N Y Acad Sci 1028:81-89.
Lovat PE, Ranalli M, Annichiarrico-Petruzzelli M, Bernassola F, Piacentini M, Malcolm AJ, Pearson ADJ, Melino G, Redfern CPF. 2000. Effector mechanisms of fenretinide-induced apoptosis in neuroblastoma. Exp Cell Res 260:50-60.
Martin S, Hill DS, Paton JC, Paton AW, Birch-Machin MA, Lovat PE, Redfern CP. 2010. Targeting GRP78 to enhance melanoma cell death. Pigment Cell Mel Res 23:675-82.
Misra UK, Mowery Y, Kaczowka S, Pizzo SV. 2009. Ligation of cancer cell surface GRP78 with antibodies directed against its COOH-terminal domain up-regulates p53 activity and promotes apoptosis. Molecular cancer therapeutics 8:1350-62.
Nishitoh H, Matsuzawa A, Tobiume K, Saegusa K, Takeda K, Inoue K, Hori S, Kakizuka A, Ichijo H. 2002. ASK1 is essential for endoplasmic reticulum stress-induced neuronal cell death triggered by expanded polyglutamine repeats. Genes Dev 16:1345-55.
Niture SK, Kaspar JW, Shen J, Jaiswal AK. 2010. Nrf2 signaling and cell survival. Toxicol Appl Pharmacol 244:37-42.
Niwa M, Sidrauski C, Kaufman RJ, Walter P. 1999. A role for presenilin-1 in nuclear accumulation of Ire1 fragments and induction of the mammalian unfolded protein response. Cell 99:691-702.
Obeng EA, Carlson LM, Gutman DM, Harrington WJ, Jr., Lee KP, Boise LH. 2006. Proteasome inhibitors induce a terminal unfolded protein response in multiple myeloma cells. Blood 107:4907-16.
Pagnan G, Di Paolo D, Carosio R, Pastorino F, Marimpietri D, Brignole C, Pezzolo A, Loi M, Galietta LJ, Piccardi F, Cilli M, Nico B, Ribatti D, Pistoia V, Ponzoni M. 2009. The combined therapeutic

effects of bortezomib and fenretinide on neuroblastoma cells involve endoplasmic reticulum stress response. Clin Cancer Res 15:1199-209.
Pincus D, Chevalier MW, Aragon T, van Anken E, Vidal SE, El-Samad H, Walter P. 2010. BiP binding to the ER-stress sensor Ire1 tunes the homeostatic behavior of the unfolded protein response. PLoS Biol 8:e1000415.
Reddy RK, Mao C, Baumeister P, Austin RC, Kaufman RJ, Lee AS. 2003. Endoplasmic reticulum chaperone protein GRP78 protects cells from apoptosis induced by topoisomerase inhibitors: role of ATP binding site in suppression of caspase-7 activation. J Biol Chem 278:20915-24.
Ritz C, Streibig JC. 2005. Bioassay Analysis using R. J Stat Software 12.
Sasagawa Y, Yamanaka K, Ogura T. 2007. ER E3 ubiquitin ligase HRD-1 and its specific partner chaperone BiP play important roles in ERAD and developmental growth in Caenorhabditis elegans. Genes to Cells 12:1063-73.
Schroder M. 2006. The unfolded protein response. Mol Biotechnol 34:279-290.
Suzuki T, Lu J, Zahed M, Kita K, Suzuki N. 2007. Reduction of GRP78 expression with siRNA activates unfolded protein response leading to apoptosis in HeLa cells. Arch Biochem Biophys 468:1-14.
Urano F, Wang X, Bertolotti A, Zhang Y, Chung P, Harding HP, Ron D. 2000. Coupling of stress in the ER to activation of JNK protein kinases by transmembrane protein kinase IRE1. Science 287:664-6.
Van Huizen R, Martindale JL, Gorospe M, Holbrook NJ. 2003. P58^{IPK}, a novel endoplasmic reticulum stress inducible protein and potential negative regulator of eIFalpha signaling. J Biol Chem 278:15558-64.
Wing X, Lawson B, Brewer JW, Zinszner H, Ron D. 1996. Signals from the stressed endoplasmic reticulum induce C/EBP-homologous protein (CHOP/GADD153). Mol Cell Biol 16:4273-80.
Yoneda T, Imaizumi K, Oono K, Yui D, Gomi F, Katayama T, Tohyama M. 2001. Activation of caspase-12, an endoplastic reticulum (ER) resident caspase, through tumor necrosis factor receptor-associated factor 2-dependent mechanism in response to the ER stress. J Biol Chem 276:13935-40.
Yoshida H, Haze K, Yanagi H, Mori K. 2000. ATF6 activated by proteolysis binds in the presence of NF-Y (CBF) directly to the cis-acting element responsible for mammalian unfolded protein response. Mol Cell Biol 20:6755-67.
Zhou H, Zhang Y, Fu Y, Chan L, Lee AS. 2011. Novel mechanism of anti-apoptotic function of 78-kDa glucose-regulated protein (GRP78): endocrine resistance factor in breast cancer, through release of B-cell lymphoma 2 (BCL-2) from BCL-2-interacting killer (BIK). The Journal of biological chemistry 286:25687-96.

Figure 1:
Response of neuroectodermal cells to fenretinide or bortezomib. A, dose-response curves for cell death after 24 h drug treatment (% apoptosis or the % cells in the subG1 fraction in flow cytometry of propidium iodide-stained cells). Open symbols and dotted lines are responses to fenretinide (dose, top axis) and filled symbols and solid lines are responses to bortezomib (dose, bottom axis). Curves are 4-parameter sigmoidal dose response curves fitted with package 'drc' in R. B, dose-dependent induction of ATF4 after 4 h treatment with fenretinide or bortezomib, expressed as amoles/cell estimated from Western blots with purified ATF4 protein fragment as standard, in response to fenretinide- (top axis) or bortezomib (bottom axis). Symbols and lines as in A.

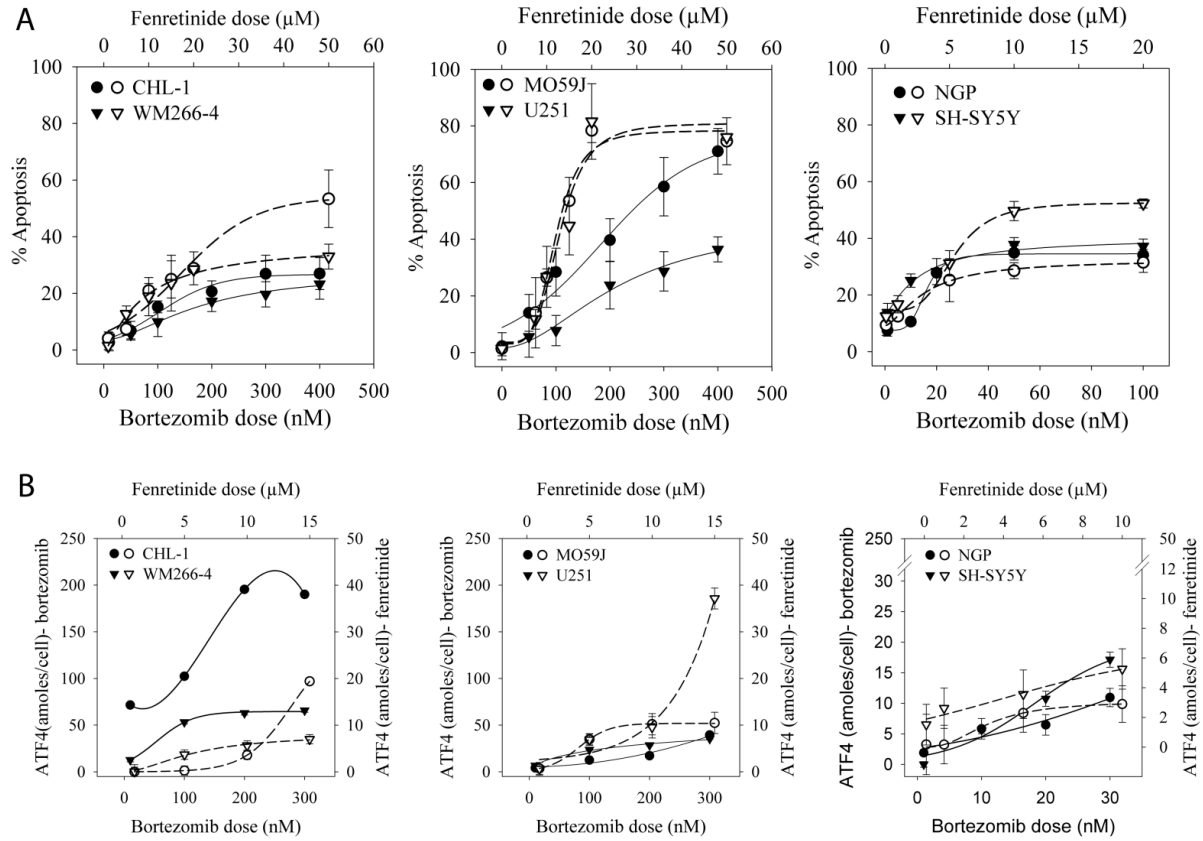

Figure 2:
Induction of stress in response to fenretinide or bortezomib. Time course of induction of ROS (vertical panel A) and ATF4 (vertical panel B) in melanoma (top graph), glioblastoma (centre graph) and neuroblastoma (bottom graph) cells treated with fenretinide (10 μM or 5 μM for melanoma/glioblastoma and neuroblastoma cells, respectively). Time courses of induction of ubiquitinated proteins (vertical panel C) and ATF4 (vertical panel D) after treatment of cell lines with bortezomib (200 nM or 20 nM for melanoma/glioblastoma and neuroblastoma cells, respectively. Examples of Western blots used for densitometric quantification of protein ubiquitination are shown in horizontal panel E. Error bars are 95% confidence intervals.

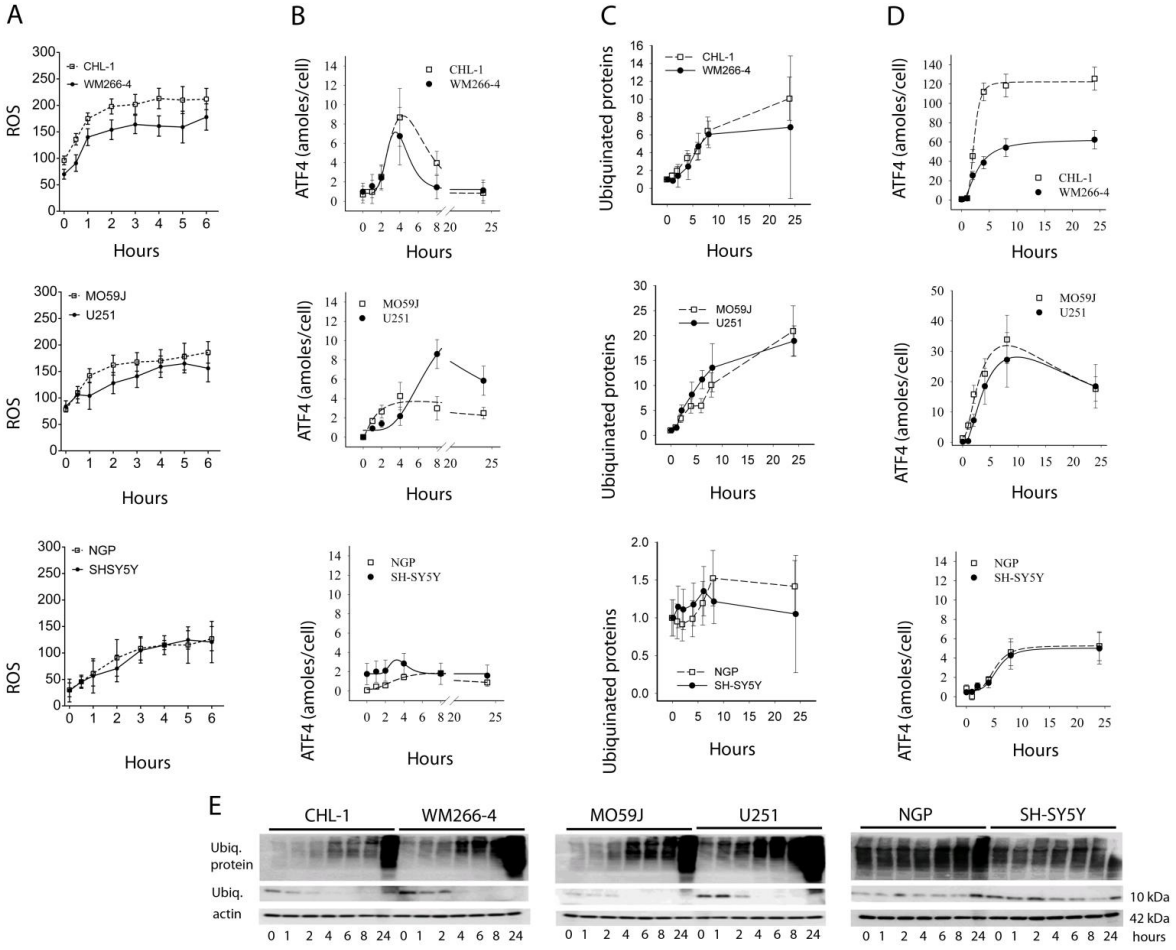

Figure 3:
SiRNA-mediated knockdown of GRP78 measured by Western blotting and densitometric quantification (left column) and sensitivity to ER-stress-induced cell death (right column). Published data for melanoma cells from the study of [Martin et al., 2010] are shown in panels A (CHL-1 cells) and B (WM266-4 cells) to facilitate comparison with MO59J (Panel c) and U251 (Panel D) glioblastoma cells, and NGP (Panel E) and SH-SY5Y (Panel F) neuroblastoma cells. . Cells were transfected with either scrambled control siRNA (left-hand group of three bars on each graph) or GRP78 siRNA (right-hand group of three bars on each graph) before treatment with control vehicle (white or open bars), fenretinide (grey bars; 10 μM or 5 μM for glioblastoma and neuroblastoma cells, respectively) or bortezomib (black bars; 200 nM or 20 nM for glioblastoma and neuroblastoma cells, respectively) for 24 h and then harvested for Western blotting and measurement of cell death. In the left-hand column, bar height is mean expression of GRP78 relative to the control-transfected and control-vehicle-treated cells and corrected for loading using the β-actin intensity; example blots are shown above each graph. For all cell lines, GRP78 expression (left-hand column) was reduced relative to a scrambled control siRNA by > 50% (one-way ANOVA, Dunnett's post hoc test, $P < 0.0001$). In the right-hand column, bar height is mean relative cell death (fold change; measured by flow cytometry) expressed relative to untreated, scrambled control-transfected cells. In glioblastoma cells, GRP78 knockdown increased death in response to fenretinide or bortezomib (across siRNA treatments, one-way ANOVA, Dunnett's post hoc test: MO59J $P < 0.0001$; U251 $P < 0.001$). There was no increased death in response to fenretinide or bortezomib after GRP78 knockdown in the neuroblastoma cells ($P>0.05$) but in SH-SY5Y cells treated with fenretinide there was a small decrease in death (one-way ANOVA; Dunnett's, $P < 0.05$). On the graphs: ***, $P <0.001$; **, $P < 0.01$; *, $P<0.05$; the direction (increase or decrease) of significant change is indicated by an arrow.

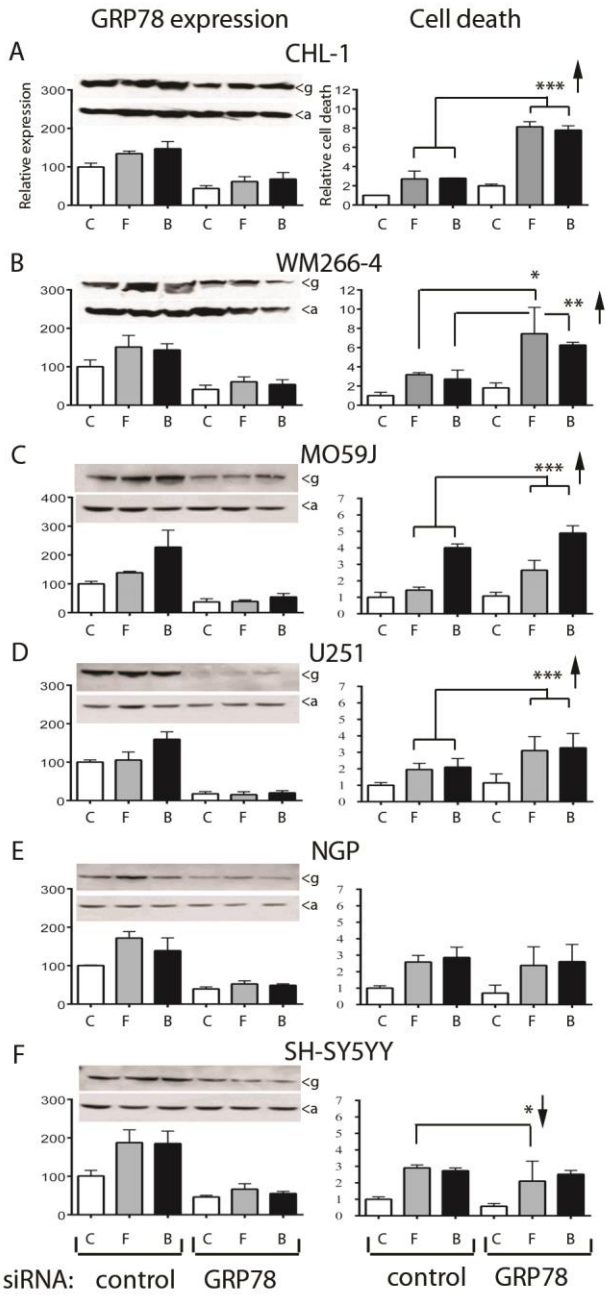

Figure 4:
Expression of the UPR activators, PERK, IRE1 and ATF6 in melanoma (A), glioblastoma (B) and neuroblastoma cells (C) after siRNA mediated knockdown of GRP78, relative to control (scrambled) siRNA-transfected cells and corrected for β-actin intensity. Example blots are shown to the right of each graph. On each graph, white/open bars are data for control transfected cells (c) and black bars are GRP78 siRNA-transfected cells (G). Data were analysed by two-way ANOVA for each cell type: initially to test the effect of treatment by cell line (main effects and interactions) for each UPR activator, and then to test the overall relative response with respect to relative UPR activator expression and treatment (main effects and interactions). The ordinate scale is from 0.5 to 1.5. For the melanoma cell lines, there was no significant effect of GRP78 knockdown on ATF6 or PERK expression (two-way ANOVA; P>0.1 and P>0.8, respectively) but a 1.3-fold increase in IRE1 expression (P=0.007; cell line and cell:treatment interactions P>0.9). UPR activator expression overall was reduced (up to 0.9-fold) in glioblastoma cells (treatment effect P=0.009; differences between UPR activator type and interactions, P>0.8). **, P < 0.01; *, P<0.05.

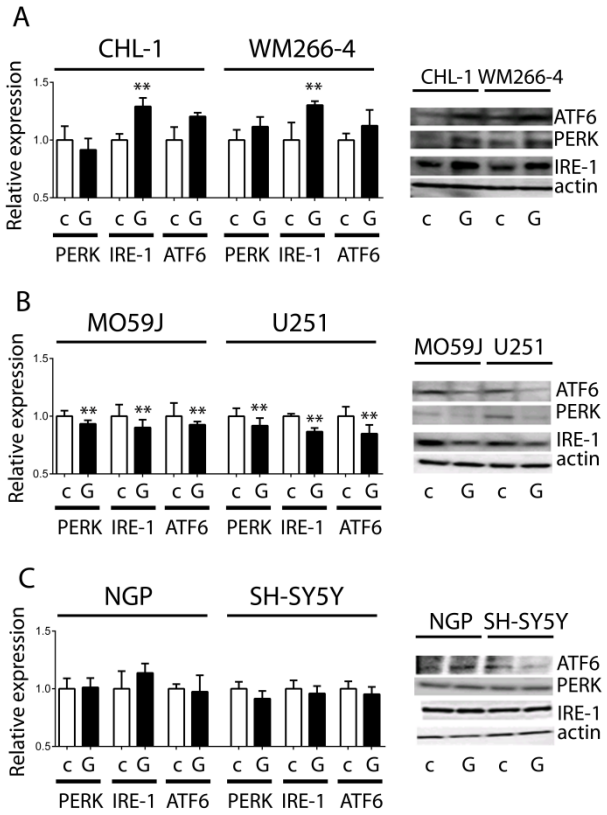

Figure 5:

Over-expression of GRP78 cDNA in a melanoma (WM266-4), glioblastoma (MO59J) and neuroblastoma cell line (NGP) stably transfected with the empty pcDNA3.0 vector or pcDNA3.1 (+) containing GRP78 cDNA (G). A, expression of GRP78 mRNA measured by quantitative real-time PCR in wild-type cells (c; open bars), vector-transfected cells (v; grey bars) and GRP78-transfected cells (G; black bars). B, expression of GRP78 protein, measured by densitometry of Western blots (details as for A) was significantly increased in all three cell lines (one-way ANOVA, F2, 54 = 65.054, P < 0.0001). C, GRP78 expression (confocal images, red signal) in wild-type WM266-4, MO59J and NGP cells (white scale bar = 20 µm), and cells stably transfected with empty vector or vector containing GRP78 cDNA. The fixed and stained cells were also stained with DAPI (blue staining) to reveal the nuclei. The staining intensity for GRP78 was significantly increased (one-way ANOVA $F_{8, 89} = 45.4$, P < 0.0001). D, Quantification of fluorescent intensities from confocal images (30 cells per condition) for wild-type, vector-transfected and GRP78-transfected WM266-4, MO59J and NGP cells (legend details as in A): there was significantly-increased staining in cells stably over-expressing GRP78 (P < 0.01) and no significant difference between the wild-type cell lines and control vector-transfected cells (P > 0.05). In all graphs, data are expressed relative to wild-type cells and the error bars are 95% CI. Images are representative of three experiments, 3 images per experiment. ***, P <0.001; **, P < 0.01; *, P<0.05.

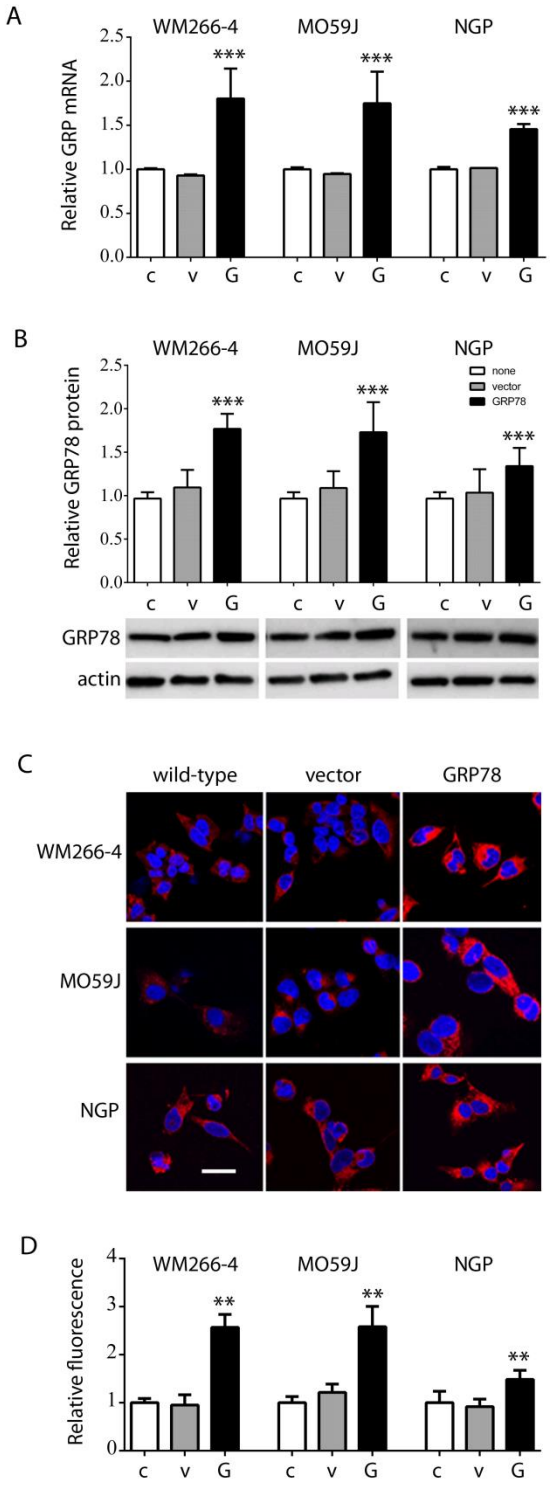

Figure 6:

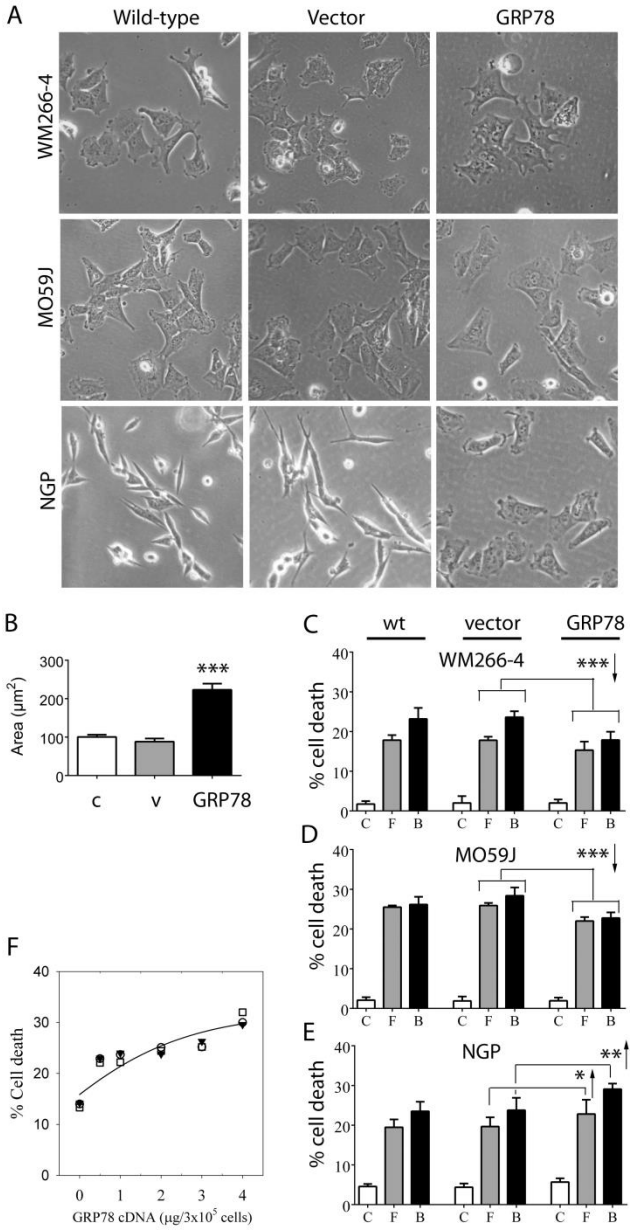

Morphology and cell death in cells over-expressing GRP78. A, phase-contrast micrographs of WM266-4 melanoma (top row), MO59J glioblastoma (middle row) and NGP neuroblastoma cells (bottom row) representing wild-type cells (left column), vector control cells (centre column) and cells stably transfected with GRP78 cDNA (right column). B, cell area in control (c; open bar), vector-transfected (v; grey bar) and GRP78-transfected (GRP78; black bar) NGP cells (one-way ANOVA, $F_{2, 29} = 62.4$, $P < 0.0001$). C, D and E, mean percentage cell death (bar heights) as measured by flow cytometry in wild-type (wt; left-hand group), vector transfected (vector; centre group) and GRP78-transfected (GRP78; right-hand group) WM266-4 (graph C), MO59J (graph D) and NGP (graph E) cells treated with control vehicle (C, open bars), fenretinide (F; grey bars; 10 μM or 5 μM for melanoma/glioblastoma and neuroblastoma cells, respectively) or bortezomib (B; black bars; 200 nM or 20 nM for melanoma/glioblastoma and neuroblastoma cells, respectively) for 24 h. GRP78 over-expression in WM266-4 and MO59J cells decreased fenretinide- or bortezomib-induced cell death (one-way ANOVA, $P < 0.0001$) but in NGP neuroblastoma cells increased sensitivity to stress (one-way ANOVA, $P < 0.01$ or $P < 0.0001$ for fenretinide or bortezomib, respectively). F, % cell death (measured by flow cytometry) in wild-type NGP cells 24 h after transient transfection with increasing amounts of GRP78 cDNA (total plasmid DNA transfected kept constant with compensating amounts of empty vector); symbols represent separate experiments. Curve is cubic function of best fit. In the absence of ER stress, GRP78 cDNA increased cell death dose-dependently (one-way ANOVA, $F_{5, 17} = 138.1$, $P < 0.0001$). Error bars are 95% CI. ***, $P < 0.001$; **, $P < 0.01$; *, $P < 0.05$; the direction (increase or decrease) of significant change is indicated by an arrow.

Figure 7:
The consequences of GRP78 over-expression: downstream markers of ER stress and cell death after treatment with ER-stress inducing drugs, and UPR activator expression in cells over-expressing GRP78 compared to wild-type cells or cells transfected with empty vector. An analysis of caspase-3 cleavage and ATF4 expression in WM266-4 (left column), MO59J (centre column) and NGP cells (right column) is shown using Western blotting in A, with densitometric quantification in B (caspase-3 cleavage) and C (ATF4 expression). Bar heights and the mean with 95% CI from 3 experiments expressed relative to control-vehicle-treated cells. Caspase-3 cleavage and ATF4 induction in response to fenretinide (F) or bortezomib (B) was reduced in WM266-4 and MO59J cells overexpressing GRP78 (one-way ANOVA for ATF4 and caspase 3 cleavage, fenretinide $P < 0.001$ or bortezomib $P < 0.001$). In NGP neuroblastoma cells over-expressing GRP78, caspase-3 cleavage was reduced compared to control vector-transfected cells ($P<0.001$) in response to fenretinide or bortezomib; conversely ATF4 induction in response to bortezomib was increased ($P < 0.0001$) but reduced in response to fenretinide treatment ($P<0.01$).. D, Western blots for UPR activator expression (PERK, IRE1 and ATF6) for the wild-type (c), vector-transfected (v) and GRP78-transfected (G) WM266-4, MO59J and NGP cells. E, Densitometric quantification, relative to wild-type cells: in WM266-4 cells over-expressing GRP78 there was a 2-fold increase in

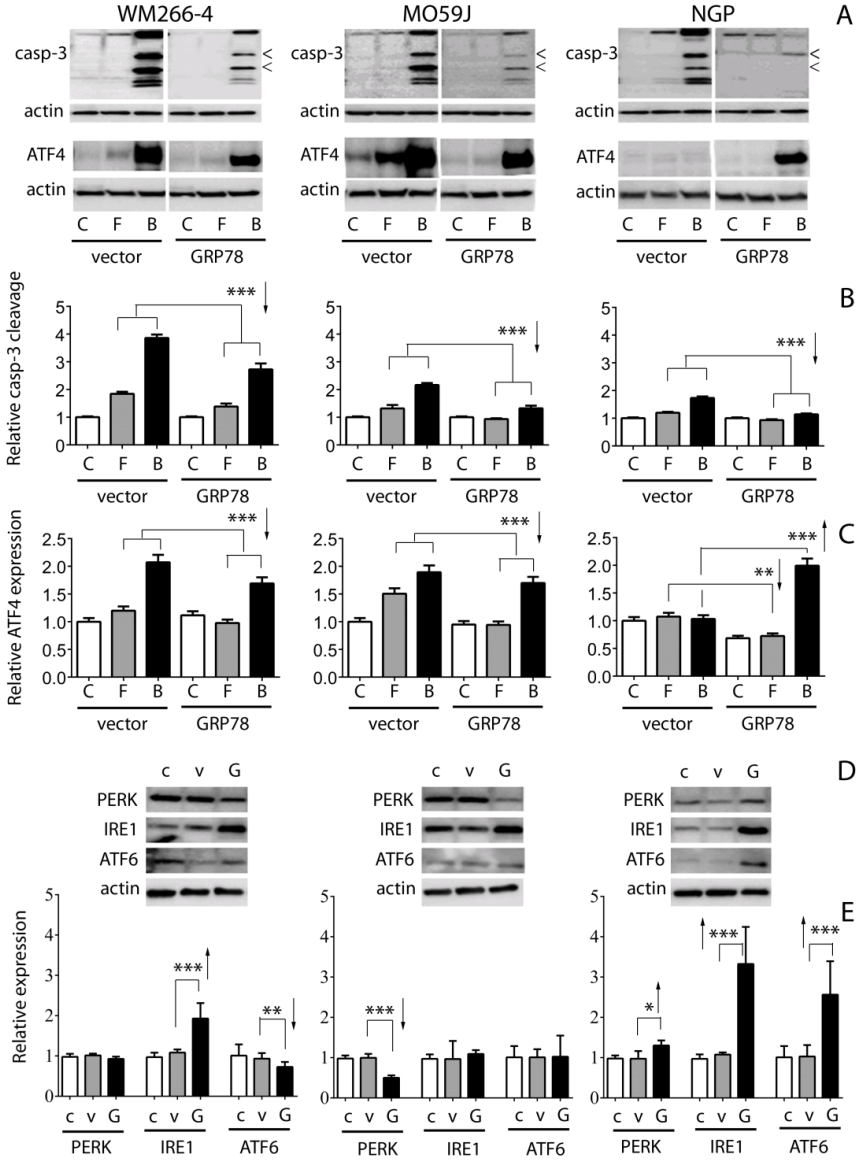

expression of IRE1 and a small decrease in ATF6 expression (one-Way ANOVA with Dunnett's, comparing stably-transfected cells to wild-type, $P < 0.0001$ for IRE1 and $P < 0.01$ for ATF6) while MO59J cells over-expressing GRP78 had a 50% reduction in PERK ($P < 0.001$). In NGP cells, over-expression of GRP78 increased levels of all three UPR activators with marked ≈3-fold increases in IRE1 and ATF6 ($P < 0.0001$) and a small increase in PERK ($P<0.05$). ***, $P <0.001$; **, $P < 0.01$; *, $P<0.05$; the direction (increase or decrease) of significant change is indicated by an arrow.

Figure 8:
Change in drug-induced stress intensity as a result of GRP78 over-expression. A, the induction of ROS 6 h after treatment of wild-type (c; open bars), vector-transfected (v; grey bars) or GRP78-over-expressing (G; black bars) cells with fenretinide (10 μM or 5 μM for melanoma/glioblastoma and neuroblastoma cells, respectively). Over-expression of GRP78 inhibited fenretinide-induced ROS in WM266-4 and MO59J cells (one-way ANOVA, $P < 0.0001$) but not in NGP neuroblastoma cells (one-way ANOVA, $P > 0.05$). B, the induction of ubiquitinated proteins 8 and 24 h after treatment of wild-type (c; open bars), vector-transfected (v; grey bars) or GRP78-over-expressing (G; black bars) cells with bortezomib (200 nM or 20 nM for melanoma/glioblastoma and neuroblastoma cells, respectively; bar heights are relative to wild-type cells). Accumulation of ubiquitin-tagged proteins was reduced by over-expression of GRP78 in WM266-4 and MO59J cells (one-way ANOVA, $P<0.05$) but increased in NGP neuroblastoma cells ($P < 0.001$). Error bars are 95% CI. ***, $P <0.001$; **, $P < 0.01$; *, $P<0.05$; the direction (increase or decrease) of significant change is indicated by an arrow.

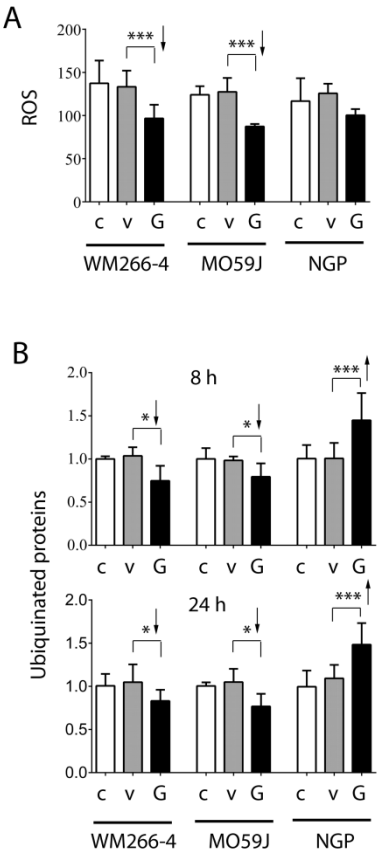

SUPPLEMENTARY DATA

FigureS1: the effect of GRP78 knockdown on cell viability.

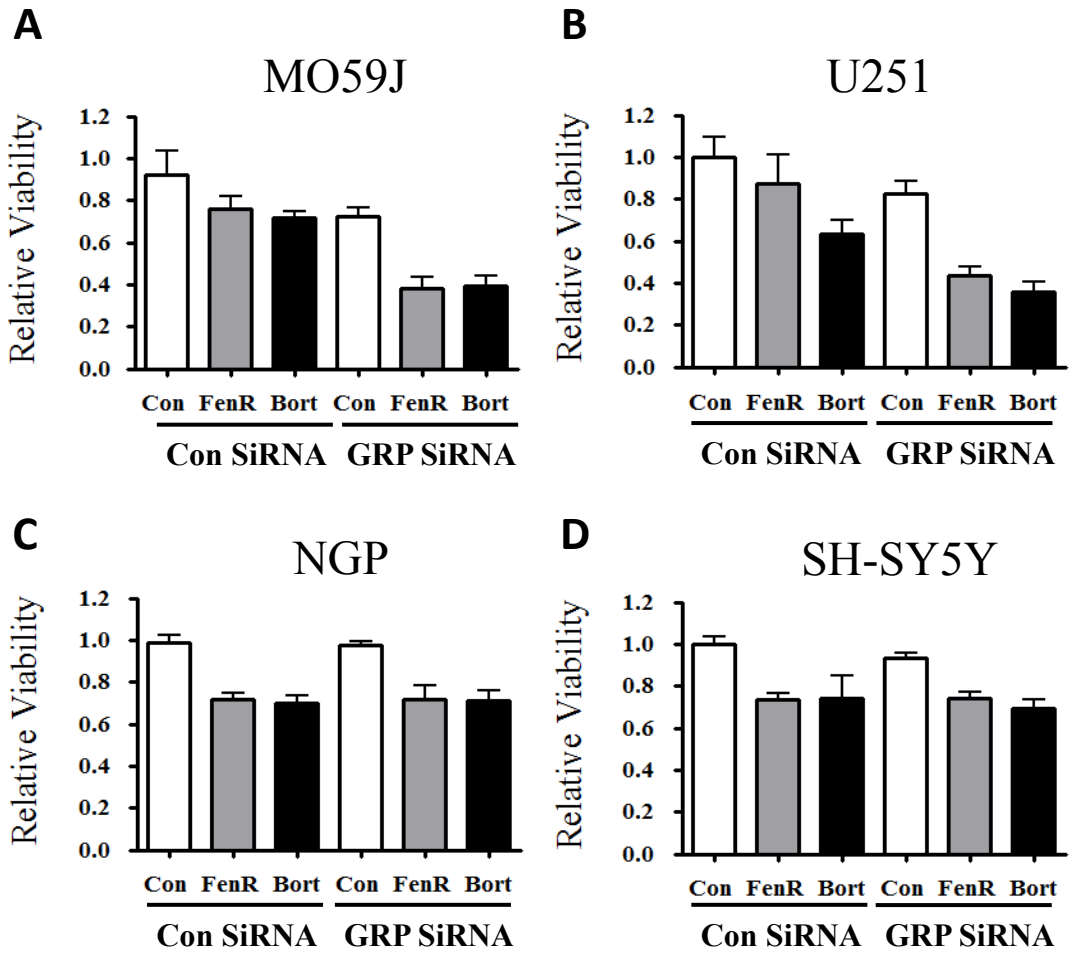

The effect of reduced GRP78 expression on sensitivity of glioblastoma and neuroblastoma cells to fenretinide and bortezomib: inhibition of cell viability. Data for CHL-1 and WM266-4 melanoma cells were published in (Martin *et al.*, 2010). A & B, MO59J and U251 glioblastoma cells, respectively; C & D, NGP and SH-SY5Y neuroblastoma cells, respectively. Cells were transfected with 40 nM GRP78 specific SiRNA (GRP78 SiRNA) in comparison to a scrambled control (Con SiRNA) prior to treating the samples with control vehicle (Con), fenretinide (FenR; grey bars; 10 µM for glioblastoma cells or 5 µM for neuroblastoma cells) or bortezomib (Bort; black bars: 200 nM for glioblastoma cells or 20 nM for neuroblastoma cells) for 24 h. Cell viability was measured using the MTS colorimetric assay. Data are expressed as the mean of 3 replicate experiments relative to control-vehicle-treated cells ± 95 % CI. Data for melanoma cells (Martin *et al.*, 2010) have been analysed together with the glioblastoma and neuroblastoma data: In melanoma and glioblastoma cells, GRP78 knock-down resulted in a significant increase in either fenretinide or bortezomib-induced inhibition of cell viability (One-way ANOVA with Dunnett's post hoc correction for CHL-1 melanoma cells and either glioblastoma cell line treated with fenretinide $P < 0.001$ or WM266-4 with fenretinide and bortezomib or CHL-1, MO59J and U251 treated with bortezomib $P < 0.0001$, respectively). Although there was an apparent reduction in cell viability in untreated cells in response to a decrease in GRP78 expression, this was not significant ($P > 0.05$). CHL-1 and WM266-4 metastatic melanoma cells also demonstrated significant differences in response ($F_{1, 47} = 10.3$, $P < 0.01$), with WM266-4 cells being less affected by GRP78 knock-down. Data for the effect of GRP78 knock-down on ER stress-induced inhibition of

neuroblastoma cell viability also demonstrated no significant differences between cells transfected with control or GRP78 specific siRNA ($P > 0.05$).

For cell viability measurments, 5000 cells per well were cultured in flat-bottomed 96-well tissue culture plates (Helena Biosciences; Gateshead, UK) in 100 µl of tissue culture medium and allowed to attach overnight before treatment. Cell viability was measured subsequently from absorbance at 490 nm in a FLUOstar Omega (BMG labtech, Aylesbury, UK) plate reader using the CellTiter 96 Aqueous One Solution reagent (Promega, Southampton, UK; MTS assay) according to the manufacturer's instructions.

Martin, S., Hill, D.S., Paton, J.C., Paton, A.W., Birch-Machin, M.A., Lovat, P.E., and Redfern, C.P.F. (2010). Targeting GRP78 to enhance melanoma cell death. Pigment Cell Mel. Res. *23*, 675-682.

Figure S2: the effect of stable GRP78 over-expression on cell viability.

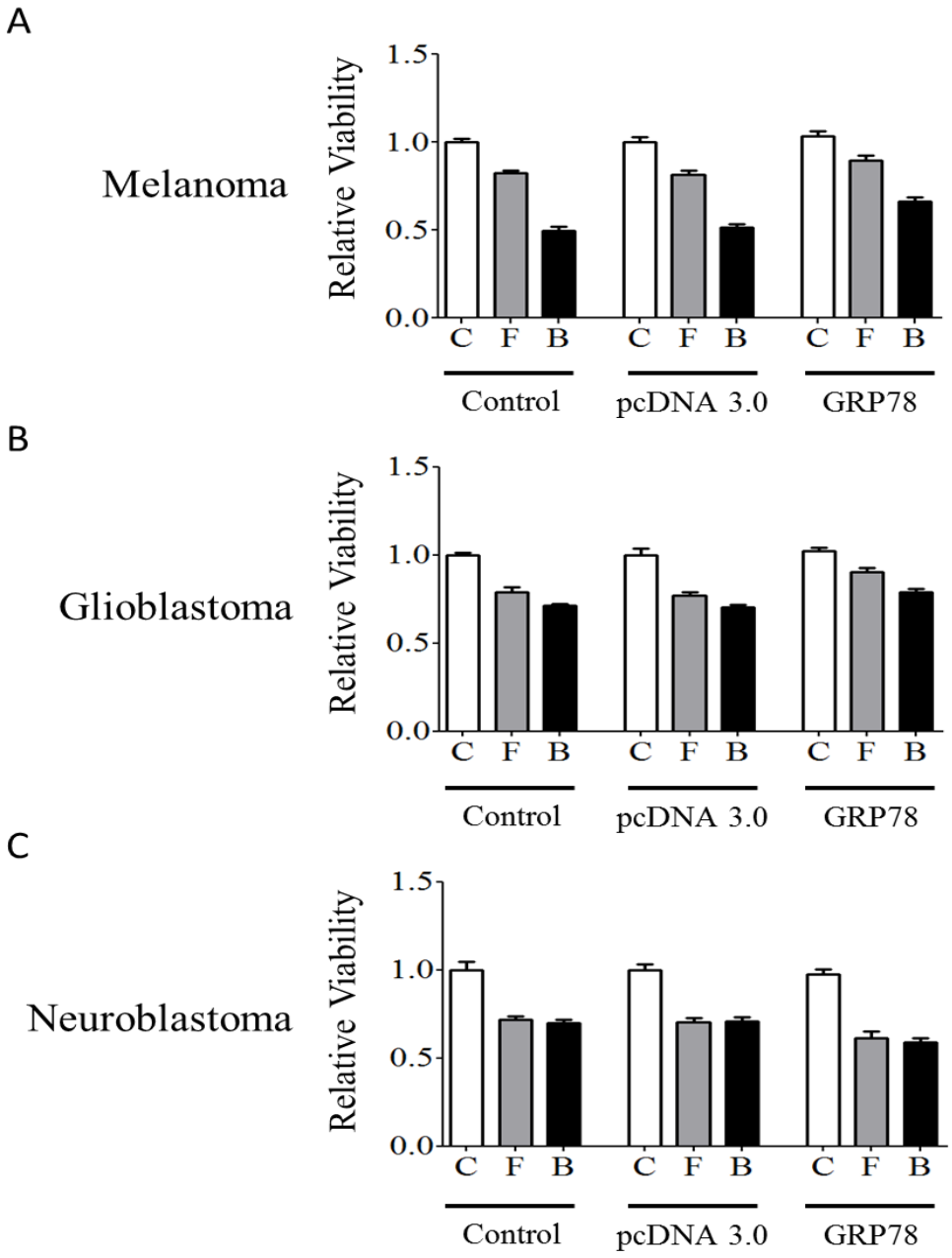

The effect of GRP78 over-expression on sensitivity to ER stress-induced inhibition of cell viability. WM266-4 melanoma (A), MO59J glioblastoma (B) and NGP neuroblastoma (C) cells: wild-type (control), stably transfected with empty vector (pcDNA3.0) or GRP78 cDNA in pcDNA3.1 were treated with control vehicle (C), fenretinide (F, 10 µM for melanoma and glioblastoma or 5 µM for neuroblastoma) or bortezomib (B, 200 nM for melanoma and glioblastoma or 20 nM for neuroblastoma) for 24 h and cell viability assessed using the MTS assay. Data were expressed as the mean values of 3 experiments of 8 individual replicates ± 95% confidence intervals. There was a significant reduction of fenretinide and bortezomib induced inhibition of cell viability in melanoma and glioblastoma cell, in comparison to controls (A & B; One-way ANOVA with Bonferroni post hoc corrections, $P < 0.0001$ for either agent, in both cancer types). Conversely, neuroblastoma cells overexpressing GRP78 showed an increase in sensitivity to ER stress (C; One-way ANOVA with Bonferroni post hoc corrections $P < 0.001$ for fenretinide and $P < 0.0001$ for bortezomib).